

GRB jets inside and outside the star: precursors and cosmological implications

Davide Lazzati, Mitchell C. Begelman

JILA, 440 UCB, University of Colorado, Boulder, CO 80309-0440, USA

Giancarlo Ghirlanda, Gabriele Ghisellini, Claudio Firmani

Osservatorio Astronomico di Brera, via E. Bianchi 46, I-23807 Merate (LC), Italy

After many years of speculation, recent observations have confirmed the association of gamma-ray bursts with core-collapse supernova explosions from massive stars. This association carries with it important consequences. The burst relativistic jet has to propagate through the cold dense stellar material before it reaches the transparency radius and the burst photons are produced. This propagation is likely to affect the initial properties of the jet, shaping it and changing its energy composition. The variability injected at the base of the jet is also likely to be erased by the jet-star interaction. Despite this, GRBs seem to have remarkably predictable properties once the radiative phase sets in, as emphasized by the recent discovery of several tight correlation between spectral, geometric and energetic properties of the jet. In this contribution we discuss the jet interaction with the star, emphasizing its time-dependent properties and the resulting energy distribution. We finally emphasize the surprising predictability of jet and radiation properties outside the star and underline its implication for standardizing the GRB candle.

I. INTRODUCTION

After many years of speculation [1, 2], the association of (at least some) long gamma-ray bursts (GRBs) with supernova (SN) explosions has been established. The first association was between GRB 980425 and SN1998bw [3]. It was a problematic and highly debated association since it implied a highly peculiar nature for GRB 980425: an event with a normal fluence but a distance 100 times smaller than other GRBs, and therefore some four orders of magnitude fainter. In addition, GRB 980425 did not have a normal afterglow in any band. Nevertheless, the peculiar nature of the SN explosion and the temporal and spatial coincidence argued strongly for the association. After GRB 980425/SN1998bw, circumstantial evidence for more associations was claimed for higher redshift events, based on the appearance of a red bump in the late afterglow light curve [4].

More recently two additional events have strengthened the association, including - at least in one case - one GRB that has all the characteristics of classical cosmological events. GRB 030329 was the brightest GRB detected by HETE-2 [5]. It had a small redshift $z = 0.168$ and multi-epoch afterglow spectroscopy revealed the emergence of a SN spectrum approximately 15 days after the burst explosion [6, 7, 8]. The spectrum and the overall supernova properties were remarkably similar to those of SN1998bw. Finally, GRB 031203, detected by INTEGRAL, looks like a twin to GRB 980425/SN1998bw [9].

The association bears new questions and riddles with it. First we know that the γ -ray photons are produced by ultra-relativistic material. The progenitor star is however dense and massive, and any outflow collecting matter geometrically from the star will be slowed-down to sub-relativistic speed very effectively.

The entrained mass can be at most a small fraction of a solar mass $M_0 \leq 5.5 \times 10^{-6} E_{51} \Gamma_2^{-1} M_\odot$. Simulations show that such a small contamination is possible (see below). The jet that reaches the surface of the star is then shaped by the interaction with the star itself. One would expect that, depending on the type of stellar progenitor, jet initial conditions and energetics, a great diversity of jets would emerge. After all type Ibc and type II supernovae show a remarkable diversity.

Even though at first sight GRB observations are characterized by a huge diversity, remarkable correlations have been discovered among jet properties. The first such correlation was discovered between the jet γ -ray energy output (not corrected for the beaming) and the break time in the afterglow light curve [10, 11]. This correlation can be understood in terms of jets with the same total energy but beamed into different opening angles [10], or in terms of structured jets with an energy distribution such that $dE/d\Omega \propto \theta^{-2}$ [12].

A further correlation was discovered between the typical frequency of photons in the prompt emission (the peak of the $\nu F(\nu)$ spectrum) and the isotropic equivalent energy output in the prompt phase [13]. According to this correlation the brighter the burst, the larger the typical frequency of photons. Finally, the tightest correlation of all was recently discovered between the typical photon energy and the beaming corrected γ -ray output [14] (under the assumption of a uniform jet). All these correlations, and especially those involving the photon frequency, have not been understood so far.

In this contribution we discuss the jet propagation inside the progenitor star [15]. We consider in particular the effect of the diminishing collimating power of the star, which is blown apart by the energy dissipated by the jet as it opens its way out of the pro-

genitor. We show that this creates time dependent effects that may be responsible for the diversity in the γ -ray phase of the burst. Such effects, however, occur on short timescales, and therefore are not relevant in the afterglow phase, which is therefore more standardized. Finally, we discuss the opportunity offered by the Ghirlanda correlation [14] to use GRBs as standard candles to constrain the expansion history of the universe at redshifts much larger than the range sampled by type Ia SNe [16].

II. THE STAR-COCOON-JET INTERACTIONS

Consider a jet generated at the core of a massive star (at a radius R_0), characterized by a luminosity L_j , an initial Lorentz factor $\Gamma_0 \gtrsim 1$, a dimensionless entropy $\eta = L_j/(\dot{M} c^2)$ (where \dot{M} is the rest mass ejection rate) and an initial opening angle θ_0 (or, alternatively, a stagnation pressure $p_{\text{stag}} = L_j \Gamma_0^2 / (4\pi c R_0^2 \theta_0^2)$). The jet attempts to propagate through the stellar material. As soon as the head of the jet reaches supersonic velocity, a double shock structure develops at the head of the jet. The speed of the head of the jet (the contact discontinuity) can be computed by balancing the pressure of the jet material with that of the cold stellar matter. Pressure balance reads [17, 18]:

$$\rho_j h_j (\Gamma \beta)_{jh}^2 c^2 + p_j = \rho_* h_* (\Gamma \beta)_h^2 c^2 + p_* \quad (1)$$

where ρ is the density, h the enthalpy and p the pressure. Subscripts are j for jet material, jh for the jet material relative to the head of the jet, h for the jet head relative to the star and $*$ for the stellar material. This equation, if we neglect the pressure terms on both sides, can be solved to give the motion of the jet head in the stellar material [17]:

$$\beta_h = \frac{\sqrt{\zeta \Gamma_j^2}}{1 + \sqrt{\zeta \Gamma_j^2}} \beta_j \quad (2)$$

where $\zeta = \rho_j h_j / \rho_*$.

The actual structure of the head of the jet is made by a contact discontinuity that separates jet material from stellar material, two thin regions of shocked material (shocked jet and shocked stellar material) and two shocks (a forward bow shock propagating into the star and a reverse shock into the jet). The shocked material is over-pressured and flows to the sides of the jet, feeding a cocoon.

The cocoon material is over-pressured with respect to both the star and the un-shocked jet. It therefore expands, driving a shock into the cold stellar material and collimating the jet until pressure balance is reached. We assume an adiabatic flow, since the jet is

optically thick inside the star. As a consequence, the Lorentz factor scales as $\Gamma_j \propto \Sigma_j^{1/2}$, where Σ_j is the area of the jet. This relation, which is valid only if dissipation is negligible, allows us to compute the jet pressure as a function only of Σ_j and to derive consequently the Lorentz factor. The cocoon evolution can be computed by applying the first law of thermodynamics:

$$d(\epsilon_c V_c) = dQ - p_c dV_c \quad (3)$$

where ϵ_c is the cocoon energy density and V_c is the volume of the cocoon. We assume that the cocoon pressure is uniform, so that p_c only depends on time. The term $dQ = L_j(1 - \beta_h)dt$ is the energy injected in the form of shocked jet material. The evolution of the cocoon volume V_c reads:

$$\frac{dV_c}{dt} = 2\pi \int_{R_0}^{R_h} R_{\perp}(r, t) v_{sh}(r, t) dr \quad (4)$$

where R_{\perp} is the transverse size of the cocoon (which is a function of radius and time) and v_{sh} is the speed of the shock driven by the cocoon pressure into the stellar material. It can be computed under the Kompaneets approximation [19] by balancing the cocoon pressure against the ram pressure exerted by the cold stellar material on the expanding cocoon: $v_{sh} = \sqrt{\epsilon_c / 3 \rho_*}$.

The above set of equations form a solvable system of differential equations. An analytic solution is not possible, especially if the time-dependent evolution of the cocoon needs to be taken into account.

To show some examples of the cocoon evolution we assume a star with mass $M_* = 15 M_{\odot}$, with radius $R_* = 10^{11}$ cm and $\rho_* \propto r^{-\alpha_*}$. Figure 1 shows the cocoon evolution at fixed times (indicated in the panels). The star has a power-law density profile $\rho_* \propto r^{-2.5}$ between 10^8 and 10^{11} cm. No funnel pre-evacuation is assumed. The jet is injected with $L_j = 10^{51}$ erg s $^{-1}$ at $r_0 = 10^8$ cm with $\theta_0 = 20^\circ$ and $\Gamma_0 = 1.5$. A recollimation shock immediately collimates and slows down the jet (upper left panel of Fig. 1). The jet emerges on the stellar surface after ~ 5 s. A total energy of 1.5×10^{51} erg has been dissipated to create the jet path into the star. Of this energy, $\sim 4 \times 10^{50}$ erg are stored into the cocoon plasma, while $\sim 10^{51}$ erg are given to the star through the cocoon shock. Such energy is of the order of the explosion energy of Ic SNe and enough to unbind the star. The jet reaches the star surface with an opening angle of $\sim 1^\circ$ and a Lorentz factor $\Gamma_{\text{br}} \simeq 24$ and is therefore in causal contact.

Figure 2 shows a similar simulation but where an exponential cutoff of the stellar density of the form $\exp[-r/(10^{10}\text{cm})]$ has been added to simulate a more realistic profile. The main effect of this change is on the shape of the cocoon that opens as the exponential cutoff is reached. Also, the jet is somewhat larger and has a larger Lorentz factor so that it turns out

to be only in marginal causal contact. These results compare positively with analytic estimates [15].

III. PRECURSORS

As the jet pierces the stellar surface, it simultaneously opens a channel for the release of the cocoon. The cocoon material therefore expands out of the star. The actual dynamics and radiative properties of the cocoon are somewhat uncertain and several different predictions have been made [20, 21, 22, 23]. What is clear is that a total energy of several $\times 10^{50}$ ergs is released almost isotropically.

Observationally, associating a precursor with a transient event is challenging, if at all possible. Attempts have been made [24, 25] adopting conservative definitions, and therefore only the tip of the iceberg was likely discovered. Figure 3 shows a sub-sample of the precursors discovered by Lazzati [25] in an analysis of ~ 100 bright long BATSE GRBs. He defined precursors as activity that is detected before the GRB trigger from the same direction as the GRB. The detected precursors are somewhat puzzling. A precursor related to the jet release or to any event that takes place before the γ -rays of the prompt phase are released is supposed to precede the GRB by:

$$\Delta T = \frac{R_\gamma}{c\Gamma^2} \sim 0.03 R_{\gamma,13} \Gamma_2^{-2} \quad \text{s} \quad (5)$$

to be compared to the several tens of seconds of delays found observationally. The only way [36] to understand these precursors as related to the cocoon breakout is to assume that the jet is initially dark in γ -rays. We argue in the following that the jet spreads during the ~ 100 s of the energy release. If the observer is not lying on the jet axis, there will be a time interval during which there will be no γ -ray emission, even though the precursor had been seen. Once the jet has spread, it enters the line of sight to the observer and becomes visible, with a delay that depends on the off-axis angle of the observer.

IV. JET BREAKOUT AND SUBSEQUENT EVOLUTION

As the jet reaches the stellar surface, it clears a channel for the cocoon. The cocoon material is therefore now free to expand out of the star and its pressure drops. We assume that from this moment on the shock between the cocoon and the cold stellar material stalls, as a consequence of the dropping cocoon pressure. This is equivalent to assuming a constant volume of the cocoon cavity inside the star. The pressure drop for the relativistic cocoon can be derived through $dE_c = -\epsilon_c \Sigma_c c_s dt$ where Σ_c is the area of the free surface through which the cocoon material

expands, ϵ_c the cocoon energy density and $c_s = c/\sqrt{3}$ is the sound speed of the relativistic gas. Writing the cocoon volume as $V_c \sim \Sigma_c r_*$, we can obtain the pressure evolution:

$$p_c = p_{c,\text{br}} \exp\left(-\frac{ct}{\sqrt{3}r_*}\right) \quad (6)$$

where $p_{c,\text{br}}$ is the cocoon pressure at the moment of shock breakout. As the cocoon pressure decreases, fresh jet material passing through the cocoon is less tightly collimated. Under isentropic conditions the jet Lorentz factor increases linearly with the opening angle and pressure balance yields $\theta_j \propto p_c^{-1/4}$, implying an exponentially increasing opening angle of the form [37]

$$\theta_j = \theta_{j,\text{br}} \exp\left[\frac{ct}{4\sqrt{3}r_*}\right]. \quad (7)$$

Dissipative jet propagation gives similar results (with merely a different numerical coefficient $\sim O(1)$ inside the exponential), provided that Γ varies roughly as a power of Σ_j .

V. JET STRUCTURE AT LARGE RADII

The angular distribution of integrated energy, as observed in the afterglow phase, is computed by integrating the instantaneous luminosity per unit solid angle from the moment the jet becomes visible along a given line of sight ($t_{\text{l.o.s.}}$) until the end of the burst:

$$\frac{dE}{d\Omega} = \int_{t_{\text{l.o.s.}}}^{T_{\text{GRB}}} \frac{dL}{d\Omega} dt \simeq \int_{t_{\text{l.o.s.}}}^{T_{\text{GRB}}} \frac{L(t)}{\pi \theta_j^2(t)} dt. \quad (8)$$

$t_{\text{l.o.s.}}$ is obtained by inverting eq. 7. Such integration is valid provided that the jet opening angle at time T_{GRB} is smaller than the natural opening angle of the jet: $T_{\text{GRB}} < 4\sqrt{3}(r_*/c) \log(\theta_0/\theta_{\text{br}})$. For the fiducial numbers assumed ($r_* = 10^{11}$ cm, $\theta_{j,\text{br}} = 1^\circ$ and $\theta_0 = 30^\circ$) this corresponds to ~ 100 s comoving burst duration. Assuming a jet with constant luminosity L and for all the lines of sight that satisfy $t_{\text{br}} < t_{\text{l.o.s.}} \ll T_{\text{GRB}}$, eq. 8 gives the jet structure

$$\frac{dE}{d\Omega} = \frac{2\sqrt{3}Lr_*}{\pi c} \theta^{-2} \quad \theta_{j,\text{br}} \leq \theta \leq \theta_0 \quad (9)$$

and $dE/d\Omega \sim \text{constant}$ inside the core radius $\theta_{j,\text{br}}$. This angular dependence, which characterizes a “structured jet” or “universal jet” [12, 27, 28, 29], is of high theoretical interest. Jets with this beam pattern reproduce afterglow observations. If the jet is powered by fall-back of material from the star to the accretion disk, the mass accretion rate would be anti-correlated with the radius of the star, for a given stellar mass.

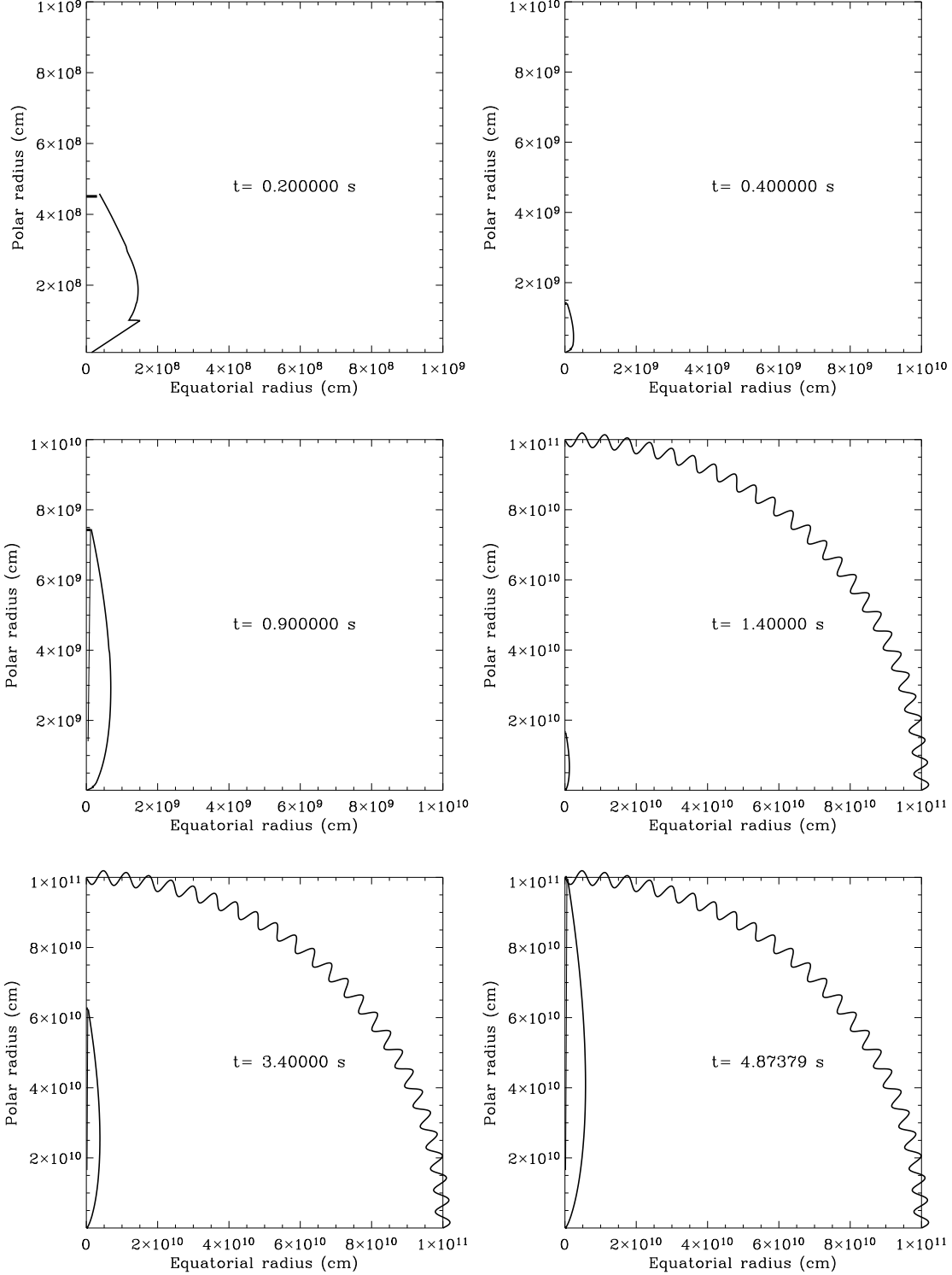


FIG. 1: Stills from a movie showing the jet and cocoon evolution inside a $15 M_{\odot}$ star with a density profile $\rho_{\star} \propto r^{-2.5}$ and a radius of 10^{11} cm. The jet is injected at a radius $r_0 = 10^8$ cm with an opening angle $\theta_0 = 20^{\circ}$, a Lorentz factor $\Gamma_0 = 1.5$ and a luminosity $L_j = 10^{51}$ erg s^{-1} . Note that the scale of figures is enlarged to emphasize the shape of the cocoon.

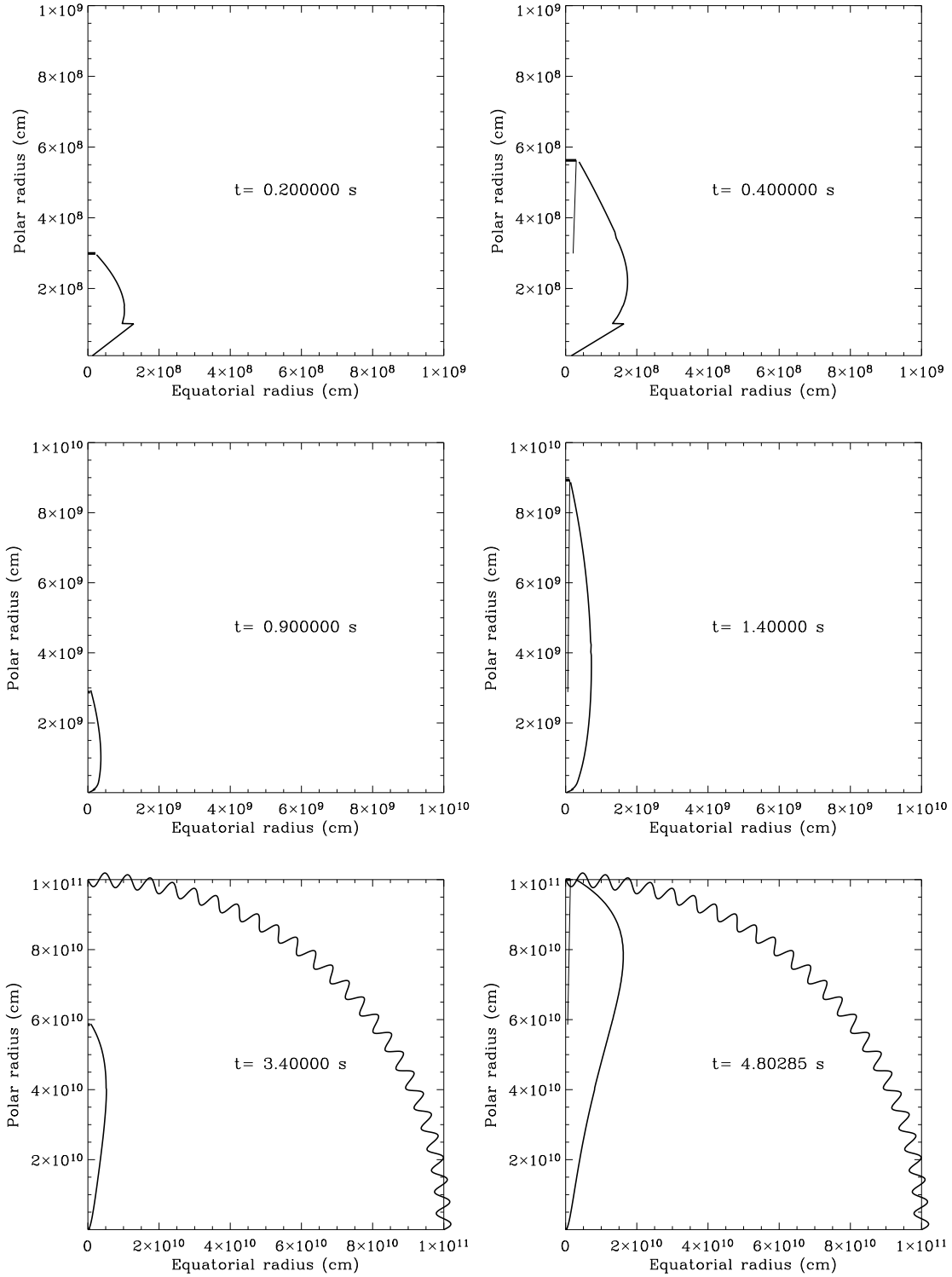


FIG. 2: Same as Fig. 1 but for a star with an exponential cutoff in the density at large radii.

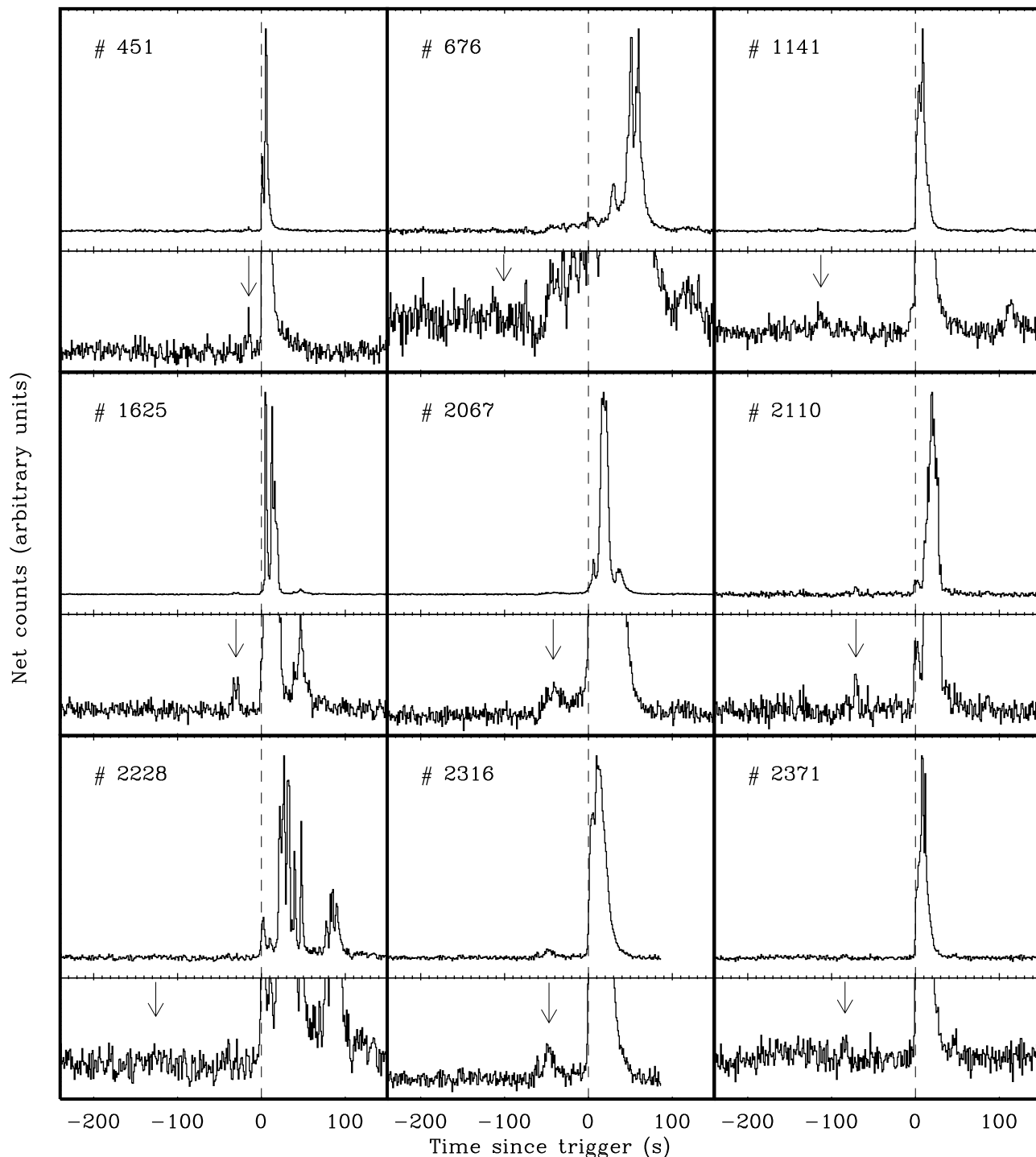


FIG. 3: Atlas of a fraction of the precursors detected in a sample of bright long BATSE GRBs [25].

In the above equations we have assumed for simplicity that the jet reaching the surface of the star is uniform. As shown by simulations [30], it is more likely that a Gaussian jet emerges from the star. On the contrary, boundary layers may be produced by the interaction of the jet with the collimating star, resulting in edge brightened jets (see the inset of Fig. 4). It can

be shown easily that the θ^{-2} pattern does not depend on the assumption of uniformity. Fig. 4 shows the integrated energy distribution for uniform, Gaussian and hollow intrinsic jets. Even though small differences are present at the edges (the jet core and the outskirts), the general behavior is always $dE/d\Omega \propto \theta^{-2}$.

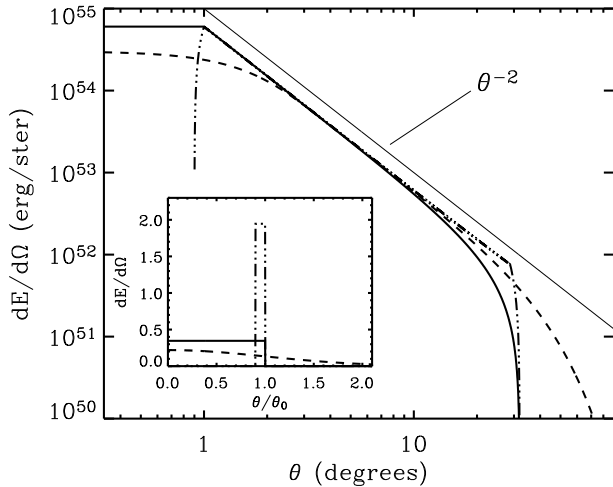


FIG. 4: Energy distribution for the afterglow phase for three instantaneous beam patterns (see inset). In all three cases a well defined $dE/d\Omega \propto \theta^{-2}$ section is clearly visible. Only the edge of the jet and its core show marginal differences. The results shown are for a jet/star with $L = 10^{51}$ erg s $^{-1}$, $T_{\text{GRB}} = 40$ s and $r_* = 10^{11}$ cm. Inset: Instantaneous beam patterns that reach the surface of the star. The solid line shows a uniform jet, dashed line shows a Gaussian energy distribution, while the dash-dotted line shows an edge brightened (or hollow) jet.

VI. THE E_γ - ϵ_{peak} CORRELATION

Correlations between observed (and intrinsic) quantities are one of the most remarkable results on the general properties of GRB jets. They tell us that, despite the varied behavior of the observed jet properties, they are not entirely random but follow a well defined path. Among such correlations [10, 11, 13] the more recent and tightest is the so-called Ghirlanda correlation [14] that finds a correspondence between the beaming corrected γ -ray energy release of the prompt emission and the typical photon frequency (the peak of the $\nu F(\nu)$ spectrum). This correlation is so tight that, within the present accuracy, it is consistent with being an exact relation. The debate is however alive on this issue [31].

The correlation is shown in Fig. 5. On the right of the same graph the Amati [13] correlation is shown for comparison. The origin of these correlation is not understood so far. It is believed that they may be due to a less dominant role of synchrotron in the prompt radiative phase of the burst [32].

VII. STANDARD CANDLES AND COSMOGRAPHY

The Ghirlanda correlation is so tight that it can be used to standardize the GRB candle [16]. If one is

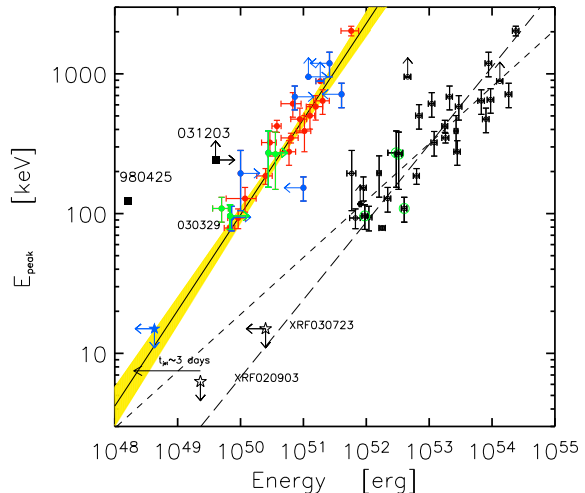


FIG. 5: Rest frame peak energy $E_{\text{peak}} = E_{\text{peak}}^{\text{obs}}(1+z)$ versus bolometric energy for the sample of GRBs with measured redshift. *Filled circles*: isotropic energy corrected for the collimation angle by the factor $(1 - \cos\theta)$, for the events for which a jet break in the light curve was observed. Grey symbols corresponds to lower/upper limits. The *Solid line* represents the best fit to the correlation, i.e. $E_{\text{peak}} \sim 480 (E_\gamma/10^{51}\text{erg})^{0.7}$ keV. *Open circles*: isotropic equivalent energy $E_{\gamma,\text{iso}}$. The *Dashed line* is the best fit to these points.

able to measure the break time of the GRB afterglow (and therefore constrain the jet opening angle) and the typical frequency of photons in the γ -ray spectrum, it is possible to predict the intrinsic energy radiated in γ -rays in the prompt phase. This allows one to measure the luminosity distance independently of redshift. If, in addition, a redshift measurement is available, we can draw a Hubble diagram and fit cosmological models to it.

Figure 6 shows the GRBs and SNe Hubble diagram before and after the empirical corrections (stretch-luminosity for SNe and Ghirlanda for GRBs). Figure 7 shows instead the constraints that can be obtained in the $\Omega_M - \Omega_\Lambda$ plane with SNe, GRBs and a simultaneous fit of the two samples [33]. Even though the simultaneous fit is clearly dominated by SNe, the perspective for GRBs, should the Ghirlanda correlation be confirmed, are very good. Their appeal is, more than to give an independent confirmation of the SNe result, to allow for an expansion to high redshift of the universe that can be sampled. This is an ideal set-up to investigate on the possible evolution of the properties of Ω_Λ to understand better the origin of dark energy.

With the launch of Swift, it is envisaged that the sample of GRBs with all the necessary data will soon become comparable to the SN sample. Fig. 8 shows a prediction of how the cosmological constraints from

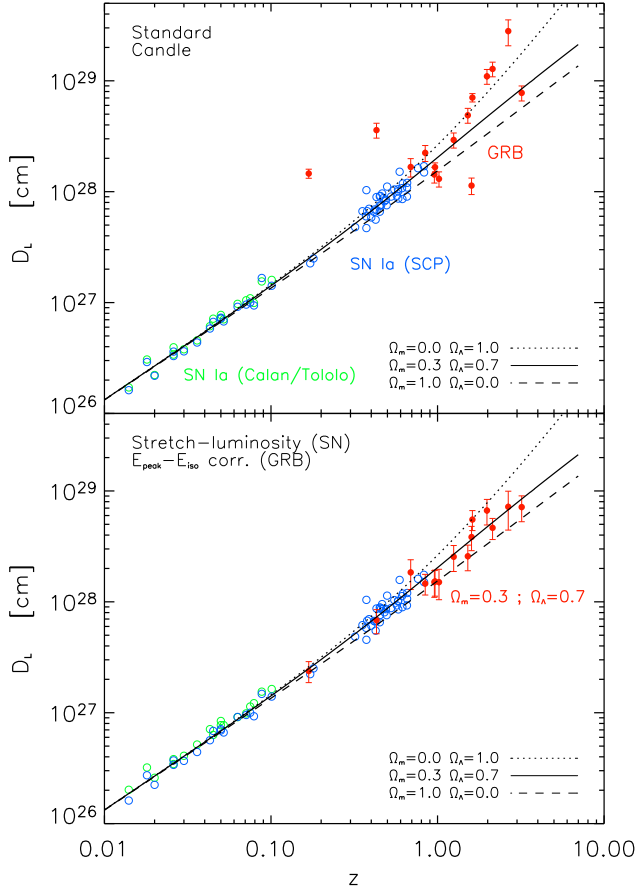


FIG. 6: Classical Hubble diagram in the form of luminosity–distance D_L vs redshift z for Supernova Ia and GRB. In the top panel the SN Ia and GRBs are treated as standard candles (no corrections applied); for GRBs $E_\gamma = 10^{51}$ erg is assumed. In the bottom panel we have applied the stretching–luminosity and the E_γ – E_{peak} relations to SN Ia and GRBs, respectively. Note that, for GRBs, the applied correction depends upon the specific assumed cosmology, here for simplicity we assume the standard $\Omega_M = 0.3$, $\Omega_\Lambda = 0.7$ cosmology. Both panels also show different $D_L(z)$ curves, as labeled.

GRBs in the Swift era may look.

VIII. DISCUSSION

We have discussed the properties of GRB jets within the framework of the GRB–SN association. We showed that the interaction of the jet with the star produces a cocoon that modifies the jet properties. Even though the jet may be released in a stationary process, with constant properties in time, the interaction with the star and the cocoon creates a time-dependent opening angle of the jet. In the prompt phase the main consequence is that the beginning of the γ -ray emission depends on the observer. In the

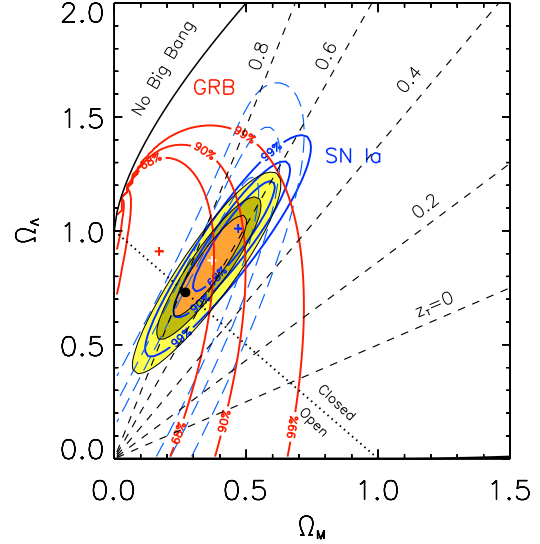
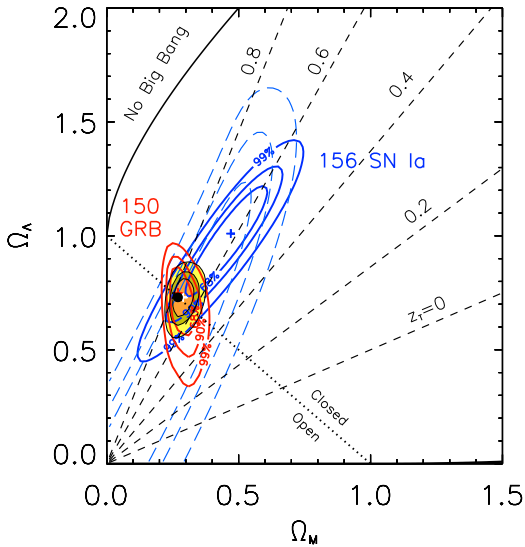


FIG. 7: Constraints in the Ω_M – Ω_Λ plane derived from our GRB sample (15 objects, red contours), from the “Gold” SN Ia sample [34] (156 objects; blue solid lines, derived assuming a fixed value of $H_0 = 65 \text{ km s}^{-1} \text{ Mpc}^{-1}$, and from the subset of SNe Ia at $z > 0.9$ (14 objects, blue long dashed lines). The three colored ellipses are the confidence regions (orange: 68%; light green: 90%; yellow: 99%) for the combined fit of type Ia SN+GRB samples. Dashed lines correspond to the changing sign of the cosmic acceleration [i.e. $q(z) = 0$] at different redshifts, as labeled. Crosses are the centers of the corresponding contours (red: GRBs; blue: SNe Ia, white: GRB+SN Ia). The black dot marks the Λ CDM cosmology. The dotted line corresponds to the statefinder $r = 1$, in this case it coincides with the flatness condition.

afterglow phase, when the time scales of the prompt emission are irrelevant, the jet is seen as a structured outflow with a well defined profile. This, with some additional constraints on the luminosity and duration of the energy injection, can create a universal jet profile [12].

Observationally, the properties of GRB jets are not independent. In particular, the Ghirlanda correlation [14] tells us that if the jet opening angle (or viewing angle) and the total energy output are known, the typical frequency of photons can be predicted. The correlation is so tight that can be used, analogously to the stretch–luminosity correlation in type Ia SN [35], to standardize the GRB candle. GRBs can therefore be used as high redshift standard candles to constrain any possible evolution in the properties of the dark energy.

Acknowledgments

FIG. 8: Swift simulated $\Omega_M - \Omega_\Lambda$ plane.

This research has been partly supported by the NSF grant AST-0307507

-
- [1] Woosley S. E., 1993, ApJ, 405, 273
[2] Paczyński B., 1998, ApJ, 494, L45
[3] Galama T. J., et al., 1998, Nature, 395, 670
[4] Zeh A., Klose S., Hartmann D. H., 2004, ApJ, 609, 952
[5] Vanderspek R., et al., 2004, ApJ, 617, 1251
[6] Stanek K. Z., et al., 2003, ApJ, 591, L17
[7] Hjorth J., et al., 2003, Nature, 423, 847
[8] Matheson T., et al., 2003, ApJ, 599, 394
[9] Malesani D., et al., 2004, ApJ, 609, L5
[10] Frail D. A., et al., 2001, ApJ, 562, L55
[11] Panaitescu A., Kumar P., 2001, ApJ, 554, 667
[12] Rossi E., Lazzati D., Rees M. J., 2002, MNRAS, 332, 945
[13] Amati L., et al., 2002, A&A, 390, 81
[14] Ghirlanda G., Ghisellini G., Lazzati D., 2004, ApJ, 616, 331
[15] Lazzati D., Begelman M. C., 2005, ApJ subm. (astro-ph/0502084)
[16] Ghirlanda G., Ghisellini G., Lazzati D., Firmani C., 2004, ApJ, 613, L13
[17] Marti J. M., Mueller E., Ibanez J. M., 1994, A&A, 281, L9
[18] Matzner C. D., 2003, MNRAS, 345, 575
[19] Kompaneets A. S., 1960, Soviet Phys. Dokl., 5, 46
[20] Mészáros P., Rees M. J., 2001, ApJ, 556, L37
[21] Ramirez-Ruiz E., MacFadyen A. I., Lazzati D., 2002, MNRAS, 331, 197
[22] Ramirez-Ruiz E., Celotti A., Rees M. J., 2002, MNRAS, 337, 1349
[23] Waxman E., Mészáros P., 2003, ApJ, 584, 390
[24] Koshut T. M., Kouveliotou C., Paciesas W. S., van Paradijs J., Pendleton G. N., Briggs M. S., Fishman G. J., Meegan C. A., 1995, ApJ, 452, 145
[25] Lazzati D., 2005, MNRAS, 357, 722
[26] Paczyński B., Haensel P., 2005, MNRAS submitted (astro-ph/0502297)
[27] Zhang B., Mészáros P., 2002, ApJ, 571, 876
[28] Salmonson J. D., 2003, ApJ, 592, 1002
[29] Lamb D. Q., Donaghy T. Q., Graziani C., 2005, ApJ, 620, 355
[30] Zhang W., Woosley S. E., MacFadyen A. I., 2003, ApJ, 586, 356
[31] Friedman A. S., Bloom J. S., 2005, ApJ submitted (astro-ph/0408413)
[32] Rees M. J., Meszaros P., 2005, ApJ submitted (astro-ph/0412702)
[33] Firmani C., Ghisellini G., Ghirlanda G., Avila-Reese V., 2005, MNRAS in press (astro-ph/0501395)
[34] Riess A. G., et al., 2004, ApJ, 607, 665
[35] Phillips M. M., 1993, ApJ, 413, L105
[36] An alternative explanation invoking the creation of a quark star has been recently put forward [26].
[37] Note that, if the jet is causally connected at breakout, the jet would freely expand to an angle $\theta_j = 1/\Gamma_{j,br} > \theta_{j,br}$ of the order of a few degrees. This would result in an initially constant opening angle. The only effect on the final energy distribution of eq. 9 is to increase the size of the jet core from $\theta_{j,br}$ to $1/\Gamma_{j,br}$.